ChemComm

Accepted Manuscript

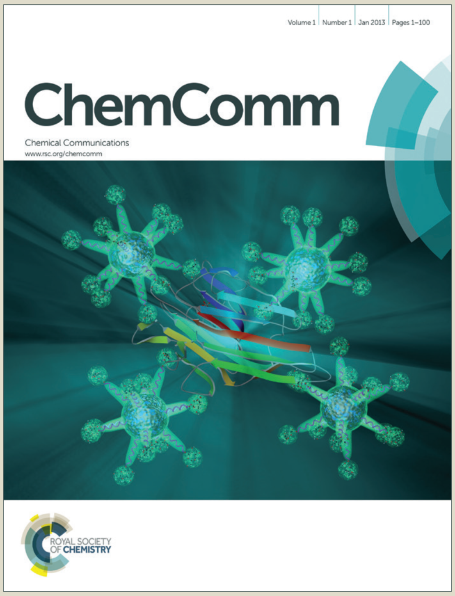

Cite this: DOI: 10.1039/c0xx00000x

www.rsc.org/xxxxxx

ARTICLE TYPE

Charge-transfer-featured materials—promising hosts for fabrication of efficient OLED through triplet harvesting via triplet fusion†

Jie Zhou,[a]‡ Ping Chen,[b]‡ Xu Wang,[c]‡ Yan Wang,[d] Yi Wang,[a] Feng Li,[b*] Minghui Yang,[d] Yan Huang,[a] Junsheng Yu,[c*] and Zhiyun Lu[a*]

Received (in XXX, XXX) Xth XXXXXXXXX 20XX, Accepted Xth XXXXXXXXX 20XX
DOI: 10.1039/b000000x

A Charge-transfer-featured naphthalimide derivative with small exchange energy but lower lying $^3\pi\pi^*$ than ^{3}CT state is found to contribute to the triplet harvesting through P-type rather than E-type delayed fluorescence, and could act as a quite promising host to achieve highly efficient OLEDs.

Owing to the low-cost together with much enhanced efficiency through triplet exciton harvesting, organic light-emitting diodes (OLEDs) based on delayed fluorescence (DF) materials have attracted significant attention recently.[1] Generally, two kinds of DF could be identified, namely, thermally activated DF (TADF, E-type DF) and triplet-fusion DF (TFDF, P-type DF). For TADF materials, their small singlet-triplet energy gaps (ΔE_{ST}) enables triplet excitons to be thermally converted into singlet ones via reverse intersystem crossing (RISC), thus the theoretical internal quantum efficiency (η_{int}) of TADF-OLED could reach 100%. Based on enormous research efforts, highly efficient TADF-OLEDs have been realized.[2] In principle, both small ΔE_{ST} and high photoluminescence quantum yield (PLQY) are essential factors for TADF emitters. Yet to achieve small ΔE_{ST}, electron and hole should be decoupled on spatially separated frontier orbitals of the compound, which would lead to intermolecular charge-transfer (ICT) transition with low possibility, hence poor PLQY.[2a] Thus the conflict between low ΔE_{ST} and high PLQY makes it difficult to develop high performance TADF materials.

On the other hand, for TFDF materials whose prerequisite is $2E_T \geq E_S$,[3] additional singlet excitons could be yielded through triplet-triplet annihilation (TTA) process, and the η_{int} of TFDF-OLEDs could reach 62.5%.[4] More importantly, the harvesting of triplet excitons could be realized not only by the emitters,[1c,1d,5] but also by the hosts via energy transfer (ET) to emitting guests.[4,6] For example, non-doped blue TFDF-OLED with maximum external quantum efficiency (η_{extmax}) of 7.18%,[1d,5a] and red doped one with η_{extmax} of 11.3%[6b] have been achieved successfully, indicating that TTA process could also contribute significantly to the improvement of efficiency in case of fluorescent OLEDs. In fact, it should be more promising if extra singlets could be produced through host rather than emitter, since intense solid state fluorescence, which is difficult to be acquired for most fluorophores due to the notorious concentration quenching, is not an indispensable factor for doping matrices.

However, most of the current investigations are focused on elucidating of the role TTA process plays in the enhancement of electroluminescence (EL) efficiency,[1c,7] while the small-molecular TF materials studied intensively are mostly limited to anthracene derivatives,[1c,1d,5b,8] Alq_3,[9] and rubrene,[10] whose S_1 and T_1 states are both of $\pi\pi^*$ character. Little attention has been paid to the TFDF character of ICT-featured compounds. Nevertheless, a recent study from Jankus et al.[11] has revealed that in an intermolecular CT exciplex system whose exchange energy is nearly zero, if $^3\pi\pi^*$ is lower lying than ^{3}CT state, it is TFDF *not* TADF process that dominates the EL, and highly efficient blue fluorescence TFDF-OLED has been achieved. Thus compounds with ICT character might not only act as TADF emitters, but also act as promising TFDF materials.

In this paper, we report on our discovery that **CzPhONI**, an ICT-featured compound with quite small exchange energy but lower lying $^3\pi\pi^*$ than ^{3}CT state, is promising TFDF- rather than TADF-OLED material. According to magneto-EL (MEL) measurement results, TTA process should dominate in OLEDs with **CzPhONI** as both non-doped emitter and doping matrix. Using it as host, an orange-red OLED with η_{extmax} of 3.59% has been achieved, which is much higher than its theoretical limited 25% singlet production (η_{extmax} : 2.50%).

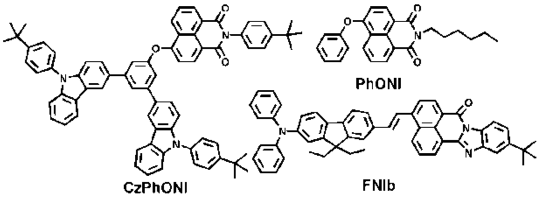

Fig. 1 Molecular structures of **CzPhONI**, **PhONI** and **FNIb**.

The molecular structure of the compounds discussed here is illustrated in Fig. 1. Because XRD characterization results reveal that the Ph and naphthalimide (NI) segments of **PhONI** are almost orthogonally twisted (Fig. S1), two electron-rich carbazyl (Cz) units are introduced to the *meta*-position of Ph segment to construct **CzPhONI**, so that electronic coupling between Cz donor and NI acceptor could be minimized. This supposition is further validated by density functional theory (DFT) calculations, since the dihedral angle between NI and Ph units is calculated to be 89.5 ° in the ground-state optimized geometry of **CzPhONI**, and the HOMO of **CzPhONI** is merely localized on the dicarbazylphenyl moiety, whereas the LUMO is only distributed on the NI unit, showing zero overlap with the HOMO (Fig. 2).

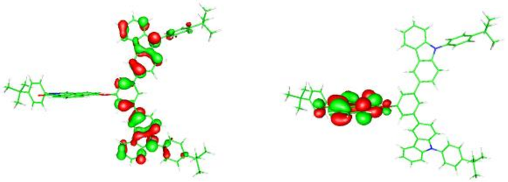

Fig. 2 The HOMO (left) and LUMO (right) of **CzPhONI** calculated at the B3LYP/6-31G(d) level.

In solution, **CzPhONI** displays two main absorption bands (Fig. S2), which could be chiefly assigned to the π-π^* transition of Cz (~300 nm)[12] and NI moieties (~360 nm),[13] respectively. No significant solvatochromism is observed, excluding the formation of ICT complex in its ground state. However, the PL emission spectrum of **CzPhONI** shows distinct solvent effect. In hexane (Hex), it displays one emission band with vibrational structure; but in more polar solvents, it exhibits dual fluorescence (Fig. 3a). In addition, the emission band with lower energy shows positive solvatochromism, and linear correlation and large slope could be discerned in the corresponding Lippert-plot (Fig. S3). Therefore, **CzPhONI** might show twisted ICT (TICT) character.[14] This deduction is verified by in-depth investigations on the PL excitation spectra, temperature effects and transient PL measurements of **CzPhONI** (Fig. S4-S7, Table S1). Furthermore, the PLQY of **CzPhONI** is much lower than that of **PhONI** (~0.8, vide Table S2), e.g., 0.02 in Hex and CCl_4, 0.01 in toluene (Tol), < 0.01 in $CHCl_3$ and dichloromethane (DCM). The very low PLQY of **CzPhONI** even in nonpolar Hex suggests the strong TICT-character of **CzPhONI**.[14] In solid film state, **CzPhONI** displays a relatively broad PL spectrum (λ_{emmax}: 493 nm) with half width of 78 nm (Fig. S7), and its PLQY is as low as 0.08, indicative of its retained CT character even in condensed state.

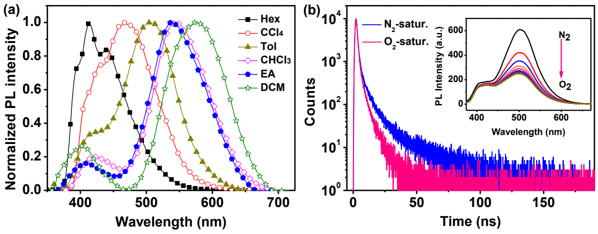

Fig. 3 (a) PL spectra of **CzPhONI** in solvents with different polarities. (b) Time-resolved PL decay traces of the TICT band of **CzPhONI** in Tol under N_2 or O_2 atmosphere (λ_{ex}=370 nm, λ_{em}=504 nm); inset: changes on PL spectrum of **CzPhONI** in Tol upon bubbling of O_2 (10 min).

As shown in Fig. 3b, in N_2-degassed Tol, the TICT emission band of **CzPhONI** displays a triple-exponential decay (τ_1=0.88 ns, 71.4%; τ_2=4.83 ns, 21.9%; τ_3=23.0 ns, 6.7%). Upon bubbling of O_2, the PL intensity of this band decreases gradually, together with much shortened decay lifetime (τ_1=0.70 ns, 66.1%; τ_2=2.24 ns, 25.7%; τ_3=6.75 ns, 8.2%). If it is the long-lived ^{3}CT state yielded via RISC process that is involved in the luminescence of TICT emission band, a much long-lived tail should be observed in the fluorescent decay curve.[2c] However, the decay lifetimes of **CzPhONI** under different conditions are relatively short, suggesting that TADF process should not dominate here.

The energy level of $^1\pi\pi^*$ (3.14 eV) and ^{1}CT (2.51 eV) states for **CzPhONI** is determined from the highest energy peak of its emission band in nonpolar Hex, and onset of the TICT band in more polar DCM, respectively;[15] while the energy of ^{3}CT state (2.46 eV) is estimated to be 50 meV below that of ^{1}CT state,[1f,11] since the exchange energy in TICT excited state should be quite small due to its spatially separated frontier orbitals.[14,2a] The lowest T_1 energy of **CzPhONI** is determined to be 2.33 eV from the onset of its phosphorescence spectrum at 77 K in DCM (Fig. S8).[2c,11] Thus the ΔE_{ST} of **CzPhONI** is calculated to be 0.18 eV. It is noteworthy that the phosphorescence spectrum of **CzPhONI** resembles that of **PhONI**, suggesting that its T_1 state should be of $^3\pi\pi^*$ character localized mainly on the NI moiety.

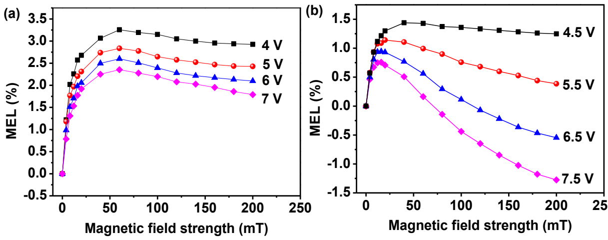

Fig. 4 The MEL of (a) Device **I**; and (b) Device **II** as a function of the external magnetic field (MEL=(*EL(B)-EL(0)*)/*EL(0)*).

The HOMO and LUMO energy levels of **CzPhONI** are estimated to be -5.64 eV and -3.14 eV respectively according to electrochemical measurements (Fig. S9). Therefore, a non-doped Device **I** with **CzPhONI** as emitter is fabricated with structure of ITO/PEDOT (35 nm)/NPB (60 nm)/**CzPhONI** (30 nm)/TPBI (40 nm)/LiF (0.8 nm)/Al, and low field MEL (≤ 0.2 T) is employed as a tool to identify if there exists RISC or TTA process in the device.[16] As shown in Fig. 4a, at applied bias of 4V (slightly higher than the turn-on voltage), the MEL of Device **I** increases sharply within low-field regime (< 50 mT), then saturates in higher B-field. Yet with increasing applied bias hence current density, after reaching the maximum value, the MEL of Device **I** decreases gradually at higher B-field strength. Accordingly, it should be TTA rather than RISC process that dominates the EL of Device **I**,[16a] despite the quite small ΔE_{ST} of **CzPhONI**. Based on the MEL and fluorescent decay results, **CzPhONI** should be a TFDF- *not* TADF-featured emitter, which is consistent with the report from Jankus et al.[11] Furthermore, to evaluate the potential of **CzPhONI** as TFDF-featured host, a doped Device **II** with structure of ITO/MoO_3 (10 nm)/NPB (35 nm)/TCTA (10 nm)/**FNIb**:**CzPhONI** (6 wt%, 30 nm)/TPBI (40 nm)/LiF (0.8 nm)/Al is also fabricated. Here, CT-featured **FNIb** is employed as the emitting dopant,[17] and the PLQY of **FNIb**:**CzPhONI** (6 wt%) doped film is determined to be 0.50. Similar to the case of Device **I**, TTA-charactered MEL responses are discerned in Device **II**, suggesting that **CzPhONI** could also contribute to the harvesting of triplet excitons through TTA-process when acts as host.

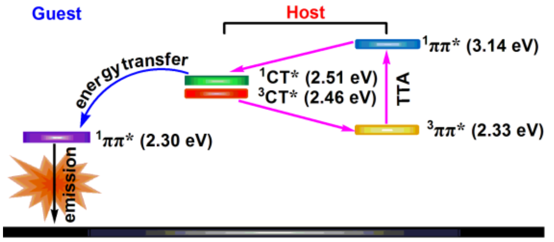

Fig. 5 Energy level diagram showing the proposed TTA and energy transfer processes in Device **II**. The energies given are for **CzPhONI**.

According to the energy level diagram, a mechanism for the TTA and ET processes within Device **II** is proposed tentatively (Fig. 5). Upon charge injection, ^{1}CT singlets are formed mainly on **CzPhONI**, which could lead to the emission of the guest through ET process. Concurrently, ^{1}CT singlets also could be transformed into ^{3}CT triplets due to their nearly degenerated energy levels. The majority of ^{3}CT triplets formed by charge recombination will be quenched by the lower lying $^3\pi\pi^*$ state of **CzPhONI**. These triplets then undergo TTA process to generate $^1\pi\pi^*$ singlets of **CzPhONI**, which could be converted to ^{1}CT via internal conversion, and so on round this loop.

Although in Device **II**, the presence of TTA process should benefit the triplet harvesting, and a maximum brightness of 7250 cd/m^2 could be achieved, its current efficiency is not satisfactory, indicating the poor carrier balance in this device (Fig. S11). To unravel which carrier is more predominant, the carrier mobility of **CzPhONI** is measured. The results indicate that **CzPhONI** posseses much higher hole mobility ($1.13\times.1^{-5}$ cm^2/V s) than electron mobility ($1.38\times.3^{-8}$ cm^2/V s). Therefore, similar with most OLEDs, holes may be the dominant charge carrier in Device **II**, hence better charge balance should be achieved if hole current is reduced. Consequently, Device **III** with structure of ITO/NPB (30 nm)/CBP (2 nm)/**FNIb**:**CzPhONI** (6 wt%, 20 nm) /Bphen (40 nm)/Mg:Ag is fabricated, in which CBP acts as hole-blocking material, Bphen with higher electron mobility than TPBI acts as electron-transporting material.[18] As depicted in Fig. 6, Device **III** is a high performance orange-red OLED with maximum current efficiency of 7.2 cd/A and brightness of 16840 cd/m^2. The EL spectra of Devices **III** and **II** are almost identical, but both slightly red-shifted and broadened relative to the PL spectrum of the emitting composite film. It is noteworthy that the η_{extmax} of Device **III** is 3.59%, which is much higher than that predicted from 25% singlet production limit (2.50%). Thus the break through of η_{extmax} in Device **III** should be attributed to the efficient harvesting of triplet excitons via TTA.

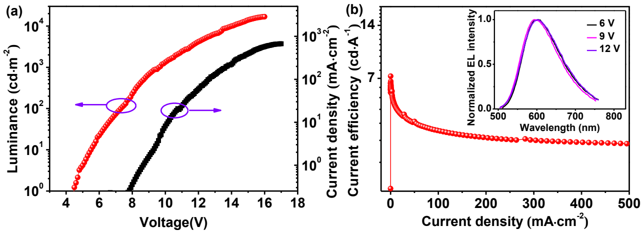

Fig. 6 (a) Current density-voltage-luminance and (b) current efficiency-current density curves of Device **III**. Inset: EL spectra of Device **III**.

In conclusion, although the ICT-featured **CzPhONI** possesses quite small exchange energy and ΔE_{ST}, its lower lying $^3\pi\pi^*$ relative to ^{3}CT state quenches TADF, but does contribute to the triplet harvesting through TTA process. More importantly, **CzPhONI** is demonstrated to be a quite promising host candidate, and OLED based on it could show high efficiency that break through the 25% singlet production limit. Our results show the importance of TFDF in producing efficient OLEDs, and may shed light on the molecular design strategy for host materials to achieve efficient OLEDs by way of P-type DF.

This work was supported by NSFC (Grant Nos. 21190031, 61177032, 61275036, 21221064, 21372168, 21373266). We also thank Analytical & Testing Center, SCU for XRD and NMR data.

Notes and references

[a] *Key Laboratory of Green Chemistry and Technology (Ministry of Education), College of Chemistry, Sichuan University, Chengdu 610064, PR China. E-mail: luzhiyun@scu.edu.cn*
[b] *State Key Laboratory of Supramolecular Structure and Materials, Jilin University, Changchun 130012, PR China. E-mail: lifeng01@jlu.edu.cn*
[c] *School of Optoelectronic Information, University of Electronic Science and Technology of China (UESTC), Chengdu 610054, PR China. E-mail: jsyu@uestc.edu.cn*
[d] *Key Laboratory of Magnetic Resonance in Biological Systems, State Key Laboratory of Magnetic Resonance and Atomic/Molecular Physics, Wuhan Institute of Physics and Mathematics, Chinese Academy of Sciences, Wuhan 430071, PR China.*

† Electronic Supplementary Information (ESI) available: Experimental details and spectropic property data. See DOI: 10.1039/b000000x/

‡ These three authors contributed equally to this work.

1 For selected examples, see: (a) G. Méhes, H. Nomura, Q. Zhang, T. Nakagawa and C. Adachi, *Angew. Chem. Int. Ed*., 2012, **51**, 11311; (b) K. Nasu, T. Nakagawa, H. Nomura, C.-J. Lin, C-H. Cheng, M-R. Tseng, T. Yasuda and C. Adachi, *Chem. Commun*., 2013, **49**, 10385; (c) C.-J. Chiang, A. Kimyonok, M. K. Etherington, G. C. Griffiths, V. Jankus, F. Turksoy and A. P. Monkman, *Adv. Funct. Mater*., 2013, **23**, 739; (d) D. Yokoyama, Y. Park, B. Kim, S. Kim, Y.-J. Pu, J. Kido and J. Park, *Appl. Phys. Lett*., 2011, **99**, 123303; (f) K. Goushi, K. Yoshida, K. Sato and C. Adachi, *Nature Photon*., 2012, **6**, 253.

2 For selected examples, see: (a) H. Uoyama, K. Goushi, K. Shizu, H. Nomura and C. Adachi, *Nature*, 2012, **492**, 234; (b) J. Li, T. Nakagawa, J. MacDonald, Q. Zhang, H. Nomura, H. Miyazaki and C. Adachi, *Adv. Mater*., 2013, **25**, 3319; (c) Q. Zhang, J. Li, K. Shizu, S. Huang, S. Hirata, H. Miyazaki and C. Adachi, *J. Am. Chem. Soc*., 2012, **134**, 14706.

3 A. P. Monkman, *ISRN Mater. Sci*., 2013, **2013**, 19.

4 Y. Zhang and S. R. Forrest, *Phys. Rev. Lett*., 2012, **108**, 267404.

5 (a) S-K. Kim, B. Yang, Y. Ma, J.-H. Lee and J.-W. Park, *J. Mater. Chem*., 2008, **18**, 3376; (b) S-K. Kim, B. Yang, Y. I. Park, Y. Ma, J-Y. Lee, H-J. Kim and J. Park, *Org. Electron*., 2009, **10**, 822.

6 (a) H. Fukagawa, T. Shimizu, N. Ohbe, S. Tokito, K. Tokumaru and H. Fujikake, *Org. Electron*., 2012, **13**, 1197; (b) D. Y. Kondakov, T. D. Pawlik, T. K. Hatwar and J. P. Spindler, *J. Appl. Phys*., 2009, **106**, 124510.

7 (a) S. M. King, M. Cass, M. Pintani, C. Coward, F. B. Dias, A. P. Monkman and M. Roberts, *J. Appl. Phys*., 2011, **109**, 074502; (b) Y. Luo and H. Aziz, *Adv. Funct. Mater*., 2010, **20**, 1285.

8 (a) R. G. Kepler, J. C. Caris, P. Avakian and E. Abramson, *Phys. Rev. Lett*., 1963, **10**, 400; (b) J. Mezyk, R. Tubino, A. Monguzzi, A. Mech and F. Meinardi, *Phys. Rev. Lett*., 2009, **102**, 087404.

9 (a) Y. L. Lei, Y. Zhang, R. Liu, P. Chen, Q. L. Song and Z. H. Xiong, *Org. Electron*., 2009, **10**, 889; (b) Y. Zhang, R. Liu, Y. L. Lei and Z. H. Xiong, *Appl. Phys. Lett*., 2009, **94**, 083307.

10 (a) A. Ryasnyanskiy and I. Biaggio, *Phys. Rev. B*, 2011, **84**, 193203; (b) I. Biaggio and P. Irkhin, *Appl. Phys. Lett*., 2013, **103**, 263301; (c) P. Irkhin and I. Biaggio, *Phys. Rev. Lett*., 2011, **107**, 017402.

11 V. Jankus, C.-J. Chiang, F. Dias and A. P. Monkman, *Adv. Mater*., 2013, **25**, 1455.

12 Y. Tao, Q. Wang, C. Yang, C. Zhong, K. Zhang, J. Qin and D. Ma, *Adv. Funct. Mater*., 2010, **20**, 304.

13 Y. Wang, X. Zhang, B. Han, J. Peng, S. Hou, Y. Huang, H. Sun, M. Xie and Z. Lu, *Dyes and Pigments*, 2010, **86**, 190.

14 Z. R. Grabowski and K. Rotkiewicz, *Chem. Rev*., 2003, **103**, 3899.

15 F. B. Dias, K. N. Bourdakos, V. Jankus, K. C. Moss, K. T. Kamtekar, V. Bhalla, J. Santos, M. R. Bryce and A. P. Monkman, *Adv. Mater*., 2013, **25**, 3707.

16 (a) P. Chen, Z. Xiong, Q. Peng, J. Bai, S. Zhang and F. Li, *Adv. Optical Mater*., 2014, **2**, 142; (b) M. Shao, L. Yan, M. Li, I. Ilia and B. Hu, *J. Mater. Chem. C*, 2013, **1**, 1330.

17 Y. Wang, J. Zhou, X. Wang, X. Zheng, Z. Lu, W. Zhang, Y. Chen, Y. Huang, X. Pu and J. Yu, *Dyes and Pigments*, 2014, **100**, 87.

18 J. H. Seo, S. J. Lee, B. M. Seo, S. J. Moon, K. H. Lee, J. K. Park, S. S. Yoon and Y. K. Kim, *Org. Electron*., 2010, **11**, 1759.